İSTANBUL TECHNICAL UNIVERSITY ★ INSTITUTE OF SCIENCE AND TECHNOLOGY

NONLINEAR LATTICE SOLITONS IN SATURABLE MEDIA

M.Sc. Thesis by
İzzet GÖKSEL

Department : **Mathematical Engineering**

Programme : **Mathematical Engineering**

JUNE 2011

İSTANBUL TECHNICAL UNIVERSITY ★ INSTITUTE OF SCIENCE AND TECHNOLOGY

NONLINEAR LATTICE SOLITONS IN SATURABLE MEDIA

M.Sc. Thesis by
İzzet GÖKSEL
(509091013)

Date of submission	:	**06 May 2011**
Date of defence examination	:	**10 June 2011**

Supervisor (Chairman)	:	**Assis. Prof. Dr. İlkay B. AKAR (İTÜ)**
Co-Supervisor	:	**Assoc. Prof. Dr. Nalan ANTAR (İTÜ)**
Members of the Examining Committee	:	**Prof. Dr. Emanullah HIZEL (İTÜ)**
		Prof. Dr. Hilmi DEMİRAY (IÜ)
		Assis. Prof. Dr. Güler AKGÜN (NKÜ)

JUNE 2011

İSTANBUL TEKNİK ÜNİVERSİTESİ ★ FEN BİLİMLERİ ENSTİTÜSÜ

**DOYURULABİLİR ORTAMLARDA DOĞRUSAL OLMAYAN
KAFES SOLİTONLARI**

**YÜKSEK LİSANS TEZİ
İzzet GÖKSEL
(509091013)**

Tezin Enstitüye Verildiği Tarih	:	**06 Mayıs 2011**
Tezin Savunulduğu Tarih	:	**10 Haziran 2011**

Tez Danışmanı	:	**Yrd. Doç. Dr. İlkay B. AKAR (İTÜ)**
Tez Eş Danışmanı	:	**Doç. Dr. Nalan ANTAR (İTÜ)**
Diğer Jüri Üyeleri	:	**Prof. Dr. Emanullah HIZEL (İTÜ)**
		Prof. Dr. Hilmi DEMİRAY (IÜ)
		Yrd. Doç. Dr. Güler AKGÜN (NKÜ)

HAZİRAN 2011

FOREWORD

First and foremost, I would like to express my gratitude to Assist. Prof. Ph.D. İlkay Bakırtaş Akar and Assoc. Prof. Ph.D. Nalan Antar for they have provided assistance in numerous ways. Our first encounter was during my undergraduate studies at an interdisciplinary summer school course about mathematical modelling and its applications which made me interested in applied mathematics. In the course of my graduate studies, they introduced me to the area concerning the topics of this work; their advises and aids throughout my studies contributed vastly to the realization of this thesis. This paper would not have been written without their guidance and supervision.

I am also grateful to TÜBİTAK for the financial support during my graduate studies.

I am tempted to individually thank all of my teachers who have shared their knowledge with me.

Last but not least, I wish to thank my family for their love and support.

I dedicate this thesis to my mother Işık.

May 2011
İzzet Göksel
(Mathematical Engineer, Computer Engineer)

TABLE OF CONTENTS

ABBREVIATIONS

CM : Center of Mass
Eq. : Equation
Fig. : Figure
NLS : Nonlinear Schrödinger
SR : Spectral Renormalization
VK : Vakhitov and Kolokolov
2D : two dimensional
(2+1)D : 2+1 dimensional

x

LIST OF FIGURES

NONLINEAR LATTICE SOLITONS IN SATURABLE MEDIA

SUMMARY

Solitons are nonlinear wave structures that are widely present in nature; they arise from fluid dynamics to biological systems and from nonlinear optics to Bose-Einstein condensates (BECs). In nonlinear optics, localized solitary waves are usually called solitons or optical modes and their existence in homogeneous and/or periodic systems is shown experimentally. In recent years, optical lattice solitons in Kerr media are deeply analyzed and it is shown that they suffer from collapse due to self-focusing or diffraction.

In this thesis, the existence and stability of optical solitons in saturable media on periodic and certain type of quasicrystal lattices (Penrose-5 and Penrose-7) are investigated.

In Section 1, the historical background of the nonlinear wave propagation in optical media is given. Basic definitions about optical lattices and medium, and the model that governs nonlinear wave propagation through a nonlinear optical lattice are also given in the same section. Since localized soliton type solutions to the model equation are found by the use of a numerical algorithm based on a double Fourier transform, this transform technique is also briefly explained.

The governing equation for the physical model that has been used in this study is the saturable nonlinear Schrödinger (NLS) equation with an external potential in (2+1)D space. This equation is given as follows:

$$iu_z(x,y,z) + u_{xx}(x,y,z) + u_{yy}(x,y,z) - \frac{e_0 u(x,y,z)}{1 + V(x,y) + |u(x,y,z)|^2} = 0 . \qquad \textbf{(0.1)}$$

In Section 2, the solution to the NLS equation with an external potential is obtained by spectral methods.

For the numerical solution of (**0.1**), a Fourier iteration method, namely the spectral renormalization method (SR) is employed which uses the ansatz $u(x,y,z) = f(x,y)e^{-i\mu z}$ where $f(x,y)$ is a complex valued function and μ is the propagation constant (eigenvalue) and solves it iteratively in the Fourier space.

In a certain parameter regime of the potential depth (V_0) and the propagation constant (μ), the first nonlinear band-gap structures are obtained for periodic and Penrose type quasicrystal potentials.

The effect of the numerical value of the saturation parameter e_0 and the potential depth V_0 to the gap width are also analyzed in detail for the above mentioned lattice types.

In Section 3, the nonlinear stability properties of the obtained solitons located in the first nonlinear gap are investigated. For this purpose, Vakhitov-Kolokolov (VK) stability criterion is explained. This criterion interprets the relation between the rate of change of the soliton power (P) with respect to the eigenvalue (μ) and the soliton stability.

This relation is often called the slope condition and used to predict collapse. In order to use the slope condition, the power versus eigenvalue graphs are depicted for the gap solitons.

The long time (distance) behavior of the fundamental solitons are also observed by direct simulations of the NLS equation, i.e. whether they conserve their shapes, locations and maximum amplitudes or not. The latter is done by means of finite differences method and a time stepping method (Runge-Kutta). The results are compared with the results that are obtained from VK criterion and their consistency is shown.

The results of the study and possible future projects are discussed in Section 4.

DOYURULABİLİR ORTAMLARDA DOĞRUSAL OLMAYAN KAFES SOLİTONLARI

ÖZET

Solitonlar, doğada bir çok yerde var olan, akışkanlar mekaniğinden biyolojik sistemlere, doğrusal olmayan optikten Bose-Einstein yoğuşmasına (BEC), birçok fiziksel olguda ortaya çıkan yapılardır. Doğrusal olmayan optikte yerel yalnız (lokalize soliter) dalgalar genellikle soliton ya da optik mod adını alırlar ve bunların deneysel olarak homojen ve/veya periyodik sistemlerdeki varlıkları gösterilmiştir. Son yıllarda optik kafes (latis) solitonları Kerr ortamlarda derinlemesine incelenmiş ve bunların odaklanmadan ötürü dalga patlaması (ya da çökmesi) nedeniyle kararlılıklarının (stabilitelerinin) bozulduğu gösterilmiştir.

Bu tezde, doyurulabilir ortamlarda periyodik ve belirli tipte yarı kristal latisler üzerinde (Penrose-5 ve Penrose-7) optik latis solitonlarının varlığı ve kararlılığı incelenmiştir.

Bölüm 1'de, optik ortamlarda doğrusal olmayan dalga yayılımının tarihsel gelişimi anlatılmıştır. Aynı bölümde optik latisler, optik ortamlar ve doğrusal olmayan optik latislerde dalga yayılımı modeli hakkında bilgiler verilmiştir. Model denklemin sayısal sonuçları Fourier dönüşümü tabanlı bir algoritma ile bulunduğu için bu dönüşüm metodu da kısaca açıklanmıştır.

Bu çalışmada kullanılan fiziksel model, (2+1) boyutlu, bir dış potansiyel içeren, doyurulabilir, doğrusal olmayan Schrödinger (NLS) denklemidir. Bu denklem aşağıdaki gibi verilir:

$$iu_z(x,y,z) + u_{xx}(x,y,z) + u_{yy}(x,y,z) - \frac{e_0 u(x,y,z)}{1 + V(x,y) + |u(x,y,z)|^2} = 0 . \qquad \textbf{(0.2)}$$

Bölüm 2'de dış potansiyel içeren doyurulabilir NLS denkleminin çözümü spektral yöntemler kulllanılarak elde edilmiştir.

(**0.2**) denkleminin sayısal çözümü, literatürde spektral renormalizasyon (SR) olarak isimlendirilen yöntem ile elde edilmiştir. Bu yöntem, $u(x,y,z) = f(x,y)e^{-i\mu z}$ yaklaşımını kullanır ve $f(x,y)$ kompleks değerli fonksiyonunu Fourier uzayında ardışık (iteratif) olarak çözer. Burada μ yayılım sabitidir (özdeğerdir).

Bu çalışmada periyodik ve Penrose tipi yarı kristal potansiyellerde, potansiyel derinliği V_0 ve yayılma sabiti μ'nün belirli değerlerinde birinci doğrusal olmayan bant yapıları bulunmuştur.

Doygunluk parametresi e_0'ın sayısal değerinin ve potansiyel derinliği V_0'ın bant genişliğine etkileri de yukarıda sözü edilen potansiyeller için ayrıntılı olarak incelenmiştir.

Bölüm 3'te birinci doğrusal olmayan yarıkta elde edilen solitonların kararlılığı ele alınmıştır. Bu amaçla öncelikle Vakhitov-Kolokolov (VK) stabilite kriteri açıklanmıştır. Bu kriter, soliton gücü (P) ile özdeğer (μ) arasındaki ilişkinin soliton kararlılığına etkisini ortaya koyar. Bu ilişki sıklıkla eğim koşulu olarak isimlendirilir ve dalga

patlamasını öngörmek için kullanılır. VK stabilite kriterinin, elde edilen kafes solitonları tarafından sağlanıp sağlanmadığını kontrol etmek amacıyla solitonların güç-özdeğer grafikleri çizilmiştir.

Temel solitonların uzun zaman (mesafe) davranışları da doyurulabilir NLS denkleminin doğrudan simülasyonuyla gözlemlenmiştir; yani solitonların şekillerini, konumlarını ve maksimum genliklerini koruyup korumadıkları kontrol edilmiştir. Son bahsedilen kontrol, sonlu farklar ve zamanda ilerleme yöntemleri (Runge-Kutta) kullanılarak yapılmıştır. Elde edilen sonuçlar, VK kriterlerinden elde edilen sonuçlarla karşılaştırılmış ve sonuçların tutarlılığı gösterilmiştir.

Çalışmanın sonuçları ve gelecekte olası projeler Bölüm 4'te tartışılmıştır.

1. INTRODUCTION

In the last few years, optical solitons have become the main area for studying solitons' interactions and they are responsible for most of the progress on soliton phenomena because of the ease with which sophisticated experiments can be conducted in a laboratory environment that offers precise control over almost every parameter. Furthermore, the ability to sample the waves directly as they propagate and the availability of numerous material systems that are fully characterized by a set of simple equations result in a field in which theory and experiments make rapid progress.

Recently, there has been considerable interest in studying solitons in systems with periodic potentials or lattices, in particular, those which can be generated in nonlinear optical materials [1, 2]. In periodic lattices, solitons can typically form when their propagation constants (or eigenvalues) are within a certain region, so called gap; a concept that is borrowed from the Floquet-Bloch theory for linear propagation. However, the external potential of complex systems can be much more general and physically richer than a periodic lattice. For example, atomic crystals can have various irregularities such as defects and edge dislocations or quasicrystal structures which have long-range orientational order but no translational symmetry [3, 4]. In general, when the lattice periodicity is slightly perturbed, the band-gap structure and soliton properties also become slightly perturbed and solitons are expected to exist in much the same way as in the perfectly periodic case [5, 6]. On one hand, little is known about the spectrum with quasi-periodic potentials [7]. On the other hand, recently in [8], NLS equation with external potentials (lattices) possessing crystal and quasicrystal structures are studied and the numerical existence of fundamental solitons is shown. In the same study, the bands and gaps of the fundamental lattice solitons are computed and their stability properties are investigated by numerical methods.

In this thesis, the existence and stability of solitons in periodic and certain quasicrystal potentials are numerically investigated. The model for this is the saturable (2+1)D nonlinear Schrödinger (NLS) equation with an external potential in three dimensional space:

$$iu_z(x,y,z) + u_{xx}(x,y,z) + u_{yy}(x,y,z) - \frac{e_0 u(x,y,z)}{1 + V(x,y) + |u(x,y,z)|^2} = 0 \ . \qquad \textbf{(1.1)}$$

In optics, $u(x,y,z)$ corresponds to the complex-valued, slowly varying amplitude of the electric field in the xy-plane propagating in the z direction, $\Delta u = u_{xx} + u_{yy}$ corresponds to diffraction, $V(x,y)$ is an external optical potential that can be written as the intensity of a sum of N phase-modulated plane waves (see [9]) and e_0 is a real constant.

For the solution of this equation, a fixed-point spectral computational method (spectral renormalization method [8]) is employed which uses the ansatz $u(x,y,z) = f(x,y)e^{-i\mu z}$ where $f(x,y)$ is a complex valued function and μ is the propagation constant (eigenvalue) and solves it iteratively in the Fourier space. Different than in the above mentioned work, the method is applied to the saturable NLS equation and therefore, it is slightly modified.

In this work, the numerical existence of fundamental solitons on the periodic and quasicrystal lattices is shown and the band-gap structures are found for periodic and Penrose type potentials firstly for fixed e_0 and then for varying e_0 and potential depth V_0 values. It is shown that band-gap structure is sensitive to the change in e_0 values, namely, gap width increases with the increasing values of e_0.

The first nonlinear gap is the edge of the parameter regime of the potential depth V_0 and eigenvalue μ for which the numerical method converges to a localized mode. In the band region, under the same potential depth V_0, beyond a certain threshold value of the eigenvalue μ, the numerical method yields an extended state which is called the *Bloch wave* region.

Next, the nonlinear stability of the fundamental solitons is investigated. For this reason, the change of the soliton power with respect to the eigenvalue (soliton power P versus μ graph) is analyzed in order to predict collapse according to the slope condition. The long time (distance) behaviors of the fundamental solitons are also observed by direct simulations of saturable NLS equation, i.e. whether they conserve their shapes, locations and maximum amplitudes or not. To study the nonlinear stability, Eq.(**1.1**) is

directly computed over a long distance (Finite difference method is used on derivatives u_{xx} and u_{yy}; fourth-order Runge-Kutta method is used to advance in z.) for both periodic and Penrose potentials. The initial conditions were fundamental solitons with %1 random noise in the amplitude and phase.

1.1 Definitions

In mathematics and physics, a *soliton* is a self-reinforcing solitary wave (a wave packet or pulse) that maintains its shape while it travels at constant speed. Solitons arise as the solutions of a widespread class of weakly nonlinear dispersive partial differential equations describing physical systems. [10]

In optics, the term soliton (also called an optical mode) is used to refer to any optical field that does not change during propagation due to a delicate balance between nonlinear and linear effects in the medium.

A *crystal* is a structure arranged in an orderly repeating pattern extending in all three spatial dimensions. Patterns are located upon the points of a *lattice*, which is an array of points repeating periodically in three dimensions. In short, a crystal is ordered and periodic (i.e. has a translational symmetry).

A structure that is ordered but non-periodic (i.e. lacks any translational symmetry) is called a *quasicrystal*. The Penrose tiling given in Fig.(1.1) is a quasicrystal, for instance and has a rotational symmetry. [11]
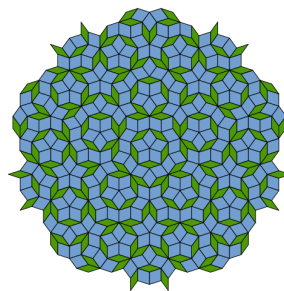
Figure 1.1: A Penrose tiling

An optical lattice is formed by the interference of counter-propagating laser beams, creating a spatially periodic polarization pattern. The resulting periodic potential can be

modelled mathematically. In this thesis, potentials of the following form will be investigated:

$$V_N(x,y) = \frac{V_0}{N^2} \left| \sum_{n=0}^{N-1} e^{i(x\cos\frac{2\pi n}{N} + y\cos\frac{2\pi n}{N})} \right| \tag{1.2}$$

The potentials for $N = 2,3,4,6$ yield periodic lattices which correspond to standard 2D crystal structures whereas $N = 5,7$ correspond to quasicrystals. In particular, the quasicrystal with $N = 5$ is often called the Penrose tiling.

In Fig.(1.2), Fig.(1.3) and Fig.(1.4), contour images, contour plots and cross sections of the lattices corresponding to $N = 4,5,7$, all with $V_0 = 1$ are displayed.
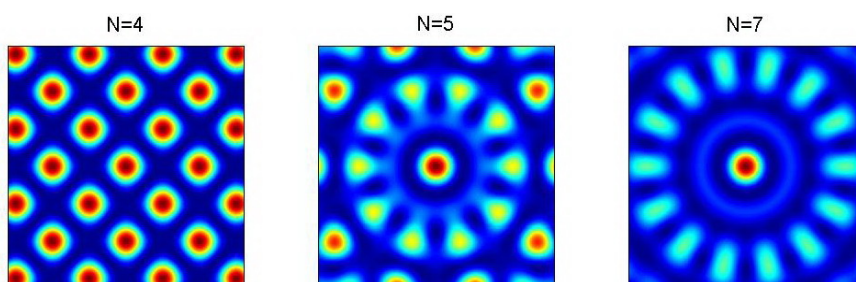
Figure 1.2: Potentials obtained from (**1.2**) by taking $N = 4,5,7$ with $V_0 = 1$
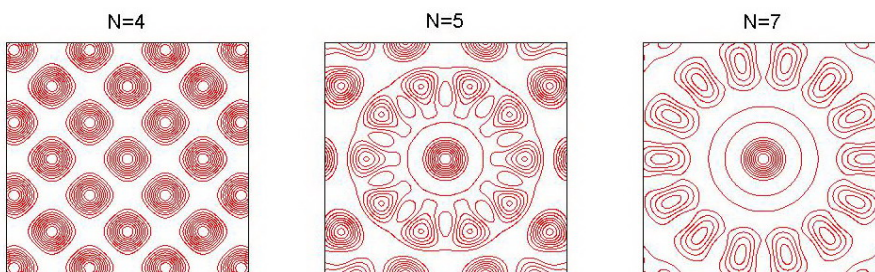
Figure 1.3: Contour plots of the potentials in Fig.(1.2)
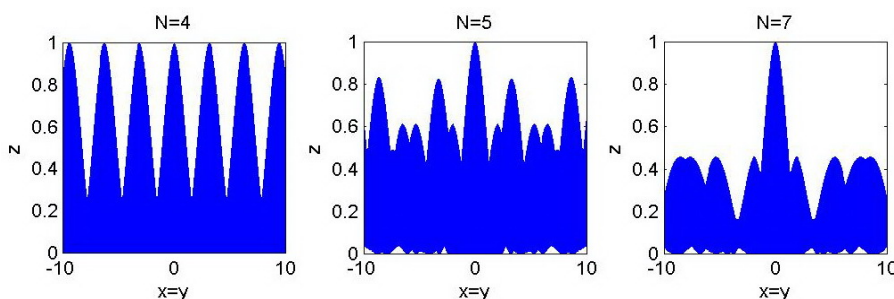
Figure 1.4: Cross sections of the potentials in Fig.(1.2)

As it can be seen from Fig.(1.4), non-periodic lattices ($N = 5$ and $N = 7$) admit only an absolute maximum unlike the periodic lattice ($N = 4$) which admits local maxima.

Recently, Freedman et al. observed solitons in Penrose and other quasicrystal lattices generated by the optical induction method [12].

1.2 Fourier Transform

For a continuous, smooth and absolutely integrable function $f(x)$, the integral transform

$$F(k_x) = \frac{1}{\sqrt{2\pi}} \int_{-\infty}^{\infty} f(x) e^{ik_x x} dx \tag{1.3}$$

is called the *Fourier transform* of $f(x)$ and conversely, the transform

$$f(x) = \frac{1}{\sqrt{2\pi}} \int_{-\infty}^{\infty} F(k_x) e^{-ik_x x} dk_x \tag{1.4}$$

is called the *inverse Fourier transform* of $F(k_x)$. [13]

The Fourier transform of f is denoted by $\mathscr{F}(f) = \hat{f}$, the inverse Fourier transform of $\hat{f}$ is denoted by $\mathscr{F}^{-1}(\hat{f})$ and clearly $\mathscr{F}^{-1}(\hat{f}) = \mathscr{F}^{-1}(\mathscr{F}(f)) = f$.

Integral transform methods are very useful for solving partial differential equations because of their properties such as linearity, shifting, scaling, etc.

Suppose that $f(x)$ tends to zero as $|x|$ tends to infinity. Then,

$$\begin{aligned} \mathscr{F}(f'(x)) &= \frac{1}{\sqrt{2\pi}} \int_{-\infty}^{\infty} f'(x) e^{ik_x x} dx \\ &= \frac{1}{\sqrt{2\pi}} \left(\left[f(x) e^{ik_x x} \right]_{-\infty}^{\infty} - ik_x \int_{-\infty}^{\infty} f(x) e^{ik_x x} dx \right) \\ &= -ik_x \mathscr{F}(f(x)). \end{aligned} \tag{1.5}$$

This result can be extended to obtain the differentiation property of the Fourier transform:

$$\mathscr{F}(f^{(n)}(x)) = (-ik_x)^n \mathscr{F}(f(x)) = (-ik_x)^n \hat{f} \ , \ \ n \in N. \tag{1.6}$$

Using this property and the linearity of the Fourier transform, one obtains the important equality

$$\mathscr{F}(\Delta f(x,y)) = \mathscr{F}(f_{xx} + f_{yy}) = -(k_x^2 + k_y^2)\hat{f} \tag{1.7}$$

which will be used during the calculations in the spectral renormalization method.

1.3 The Saturable Nonlinear Schrödinger Equation

In isotropic (Kerr) media, where the nonlinear response of the material depends cubically on the applied field, the dynamics of a quasi-monochromatic optical pulse are governed by the (2+1)D NLS equation

$$iu_z + \lambda(u_{xx} + u_{yy}) + \gamma|u|^2 u = 0 . \qquad (1.8)$$

In this model, $u(x,y,z)$ is the amplitude of the envelope of the optical beam, z is the distance in the direction of propagation, and x and y are transverse spatial coordinates.

Although higher dimensional NLS models are not integrable, they possess stationary solutions which are unstable on propagation. Maybe the most fascinating issue related to the higher dimensional NLS is that for a wide range of initial conditions, the system evolution shows collapse [14]. Wave collapse occurs where the solution tends to infinity in finite time (distance). Collapse was theoretically predicted for the (2+1)D NLS equation back in the 1960's [15].

It is known that there exist solutions of (1.8) which have a singularity in finite time and are extremely sensitive to the addition of small perturbations to the equation and there has been much interest in the determination of the structure of this singularity [16, 17].

Therefore, an important challenge in nonlinear science is to find out mechanisms arresting wave collapse in NLS models. One way of arresting collapse is adding a defocusing term to the classical (2+1)D NLS equation (1.8). Then, the equation becomes (for $\lambda = \gamma = 1$)

$$iu_z + \Delta u + |u|^2 u - Vu = 0 . \qquad (1.9)$$

In optics, $u(x,y,z)$ corresponds to the complex-valued, slowly varying amplitude of the electric field in the xy-plane propagating in the z direction, $\Delta u \equiv u_{xx} + u_{yy}$ corresponds to diffraction, the cubic term in u originates from the nonlinear (Kerr) change of the refractive index and $V(x,y)$ is an external optical potential that acts as a defocusing mechanism.

In [8], the nonlinear stability properties of the fundamental Penrose lattice solitons corresponding to $N = 5$ are investigated and shown that solitons located on lattice maxima (for both periodic and Penrose lattices) and some Penrose solitons located on lattice minima (depending on the topology of the minima) are nonlinearly unstable. In another study ([18]), the existence and nonlinear stability properties of the fundamental Penrose lattice solitons for $N = 7$ are investigated and some Penrose-7 solitons are found to be unstable depending on the location, eigenvalue and potential depth.

Optical spatial solitons and their interactions in Kerr and saturable media have been elucidated in detail in [19]. In [20], the numerical existence of an optical lattice soliton in saturable media is demonstrated by means of the spectral renormalization method. Numerical existence of vortex solitons are also reported in saturable media in [21].

It is well known that the nonlinear saturation suppresses the collapse of the fundamental solitons in two and three dimensions [22, 23].

In this work, in the light of the previous studies and with the intention of achieving stable solitons in quasicrystal type lattices, namely Penrose-5 and Penrose-7, saturable nonlinear Schrödinger equation with an external potential will be considered:

$$iu_z + \Delta u - \frac{e_0 u}{1 + V + |u|^2} = 0 \;. \tag{1.10}$$

Here, $\frac{e_0 u}{1+V+|u|^2}$ is the term for nonlinear saturation whereas e_0 is a real constant.

2. NUMERICAL EXISTENCE OF FUNDAMENTAL LATTICE SOLITONS

In this section, numerical solution to the saturable NLS equation with an external potential given in (**1.1**) will be obtained by the spectral renormalization method and the first nonlinear gap edges will be demonstrated for various types of lattices.

Firstly, the spectral renormalization method for the saturable NLS equation is explained. Secondly, gaps, (i.e. intervals of convergence) are found for different e_0 values and potentials (periodic and Penrose type). Finally, the effects of e_0 and the potential depth V_0 on the gap width are discussed.

2.1 Spectral Renormalization Method

Spectral renormalization method is essentially a Fourier iteration method. The idea of this method was proposed by Petviashvili in [24]. Later, this method is improved by Ablowitz et al. and applied to (2+1)D NLS equation [25]. In this subsection, the method is configured so that it can be applied to the saturable NLS equation.

Consider the saturable (2+1)D nonlinear Schrödinger equation with a potential in three dimensional space:

$$iu_z(x,y,z) + u_{xx}(x,y,z) + u_{yy}(x,y,z) - \frac{e_0 u(x,y,z)}{1 + V(x,y) + |u(x,y,z)|^2} = 0 \tag{2.1}$$

Using the ansatz $u(x,y,z) = f(x,y)e^{-i\mu z}$ gives

$$\mu f e^{-i\mu z} + (f_{xx} + f_{yy})e^{-i\mu z} - \frac{e_0 f e^{-i\mu z}}{1 + V + |f|^2} = 0 . \tag{2.2}$$

Multiplying both sides of this equation by $e^{i\mu z}$ results in

$$\mu f + f_{xx} + f_{yy} - \frac{e_0 f}{1 + V + |f|^2} = 0 . \tag{2.3}$$

By applying Fourier transformation, one obtains

$$\mu \hat{f} - (k_x^2 + k_y^2)\hat{f} - \mathscr{F}\left(\frac{e_0 f}{1 + V + |f|^2}\right) = 0 . \tag{2.4}$$

To prevent singularities in the denominator in future calculations, the term $r\hat{f}$ is added to and substracted from (**2.4**):

$$(\mu + r)\hat{f} - (k_x^2 + k_y^2 + r)\hat{f} - \mathscr{F}\left(\frac{e_0 f}{1 + V + |f|^2}\right) = 0 \,. \tag{2.5}$$

Solving for the $\hat{f}$ in the second term above yields

$$\hat{f} = \frac{(\mu + r)\hat{f} - \mathscr{F}\left(\frac{e_0 f}{1 + V + |f|^2}\right)}{k_x^2 + k_y^2 + r} \,. \tag{2.6}$$

Making the substitution $f(x,y) = \lambda w(x,y)$ where λ is a non-zero constant gives

$$\lambda \hat{w} = \frac{(\mu + r)\lambda \hat{w} - \mathscr{F}\left(\frac{e_0 \lambda w}{1 + V + |\lambda|^2 |w|^2}\right)}{k_x^2 + k_y^2 + r} \,. \tag{2.7}$$

Dividing by λ yields

$$\hat{w} = \frac{(\mu + r)\hat{w} - \mathscr{F}\left(\frac{e_0 w}{1 + V + |\lambda|^2 |w|^2}\right)}{k_x^2 + k_y^2 + r} \,. \tag{2.8}$$

When indexed, (**2.8**) can be utilized in an iterative method in order to find w. For this purpose, $\hat{w}$ can be calculated using the following iteration scheme:

$$\hat{w}_n = \frac{(\mu + r)\hat{w}_{n-1} - \mathscr{F}\left(\frac{e_0 w_{n-1}}{1 + V + |\lambda|^2 |w_{n-1}|^2}\right)}{k_x^2 + k_y^2 + r} \,, \quad n \in \mathbb{Z}^+ \tag{2.9}$$

with the initial condition taken as a Gaussian type function (see Fig.(2.1))

$$w_0 = e^{-((x-x_0)^2 + (y-y_0)^2)} \tag{2.10}$$

and the stopping criteria $|w_n - w_{n-1}| < 10^{-8}$. Here, the values of x_0 and y_0 define the location of the initial condition. In order to center the initial condition on the lattice maximum (the one that appears at the center of the lattice), one should e.g. take $x_0 = y_0 = 0$ and to center the initial condition on a lattice minimum (usually taken as one of the closest minima to the central maximum), one should take $x_0 = \pi, \;\; y_0 = 0$, for the periodic lattice $N = 4$.

However, λ is unknown and hence must be calculated for each iteration.

Multiplying (**2.8**) by $k_x^2 + k_y^2 + r$ leads to

$$(k_x^2 + k_y^2 + r)\hat{w} = (\mu + r)\hat{w} - \mathscr{F}\left(\frac{e_0 w}{1 + V + |\lambda|^2 |w|^2}\right) \,. \tag{2.11}$$
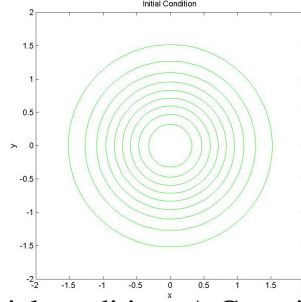
10

Figure 2.1: Initial condition: A Gaussian type function

After moving all terms to the left side, one has

$$(k_x^2 + k_y^2 - \mu)\hat{w} + \mathscr{F}\left(\frac{e_0 w}{1 + V + |\lambda|^2 |w|^2}\right) = 0 . \tag{2.12}$$

Multiplying by the conjugate of $\hat{w}$, i.e. by $\hat{w}^*$ results in

$$(k_x^2 + k_y^2 - \mu)|\hat{w}|^2 + \mathscr{F}\left(\frac{e_0 w}{1 + V + |\lambda|^2 |w|^2}\right)\hat{w}^* = 0 . \tag{2.13}$$

Finally, by integrating this equation, one gets

$$\int\int (k_x^2 + k_y^2 - \mu)|\hat{w}|^2 dk + \int\int \mathscr{F}\left(\frac{e_0 w}{1 + V + |\lambda|^2 |w|^2}\right)\hat{w}^* dk = 0 . \tag{2.14}$$

This is nothing but an equation of the form $F(\lambda) = 0$ which can be solved for λ by employing the Newton-Raphson Method, for instance. The Newton-Raphson Method is a numerical method for finding roots of equations and is given by the following iteration scheme:

$$\lambda_n = \lambda_{n-1} - \frac{F(\lambda_{n-1})}{F'(\lambda_{n-1})} \quad , \quad n \in Z^+ \tag{2.15}$$

where $F' = \dfrac{dF}{d\lambda}$ and λ_0 is the initial guess for the root.

Here

$$F(\lambda) = \int\int (k_x^2 + k_y^2 - \mu)|\hat{w}|^2 dk + \int\int \mathscr{F}\left(\frac{e_0 w}{1 + V + \lambda^2 |w|^2}\right)\hat{w}^* dk , \tag{2.16}$$

$$F'(\lambda) = \int\int (-2\lambda)\mathscr{F}\left(\frac{e_0 w|w|^2}{(1 + V + \lambda^2 |w|^2)^2}\right)\hat{w}^* dk , \tag{2.17}$$

$\lambda_0 = 1$ and the stopping criteria is $|\lambda_n - \lambda_{n-1}| < 10^{-8}$.

Once $\hat{w}$ is obtained from (**2.9**) by means of (**2.15**) to calculate λ for each iteration, the desired soliton is $f(x,y) = \lambda w(x,y) = \lambda\mathscr{F}^{-1}(\hat{w})$.

2.2 Properties of Fundamental Solitons

In this subsection, fundamental lattice solitons obtained by means of the spectral renormalization method will be demonstrated. Solitons located on lattice maxima and minima will be investigated separately. A comparison of the amplitudes and the profiles of the solitons obtained on each lattice maxima and an observation of the effect of the increment of potential depth V_0 on the periodic lattice are also analyzed in this subsection.

2.2.1 Solitons on lattice maximum

In this subsection, solitons located on the maxima of the periodic and Penrose type lattices are demonstrated.

In Fig.(2.2), 3D view of the soliton obtained on the lattice maximum with the parameters $e_0 = 8$, potential depth $V_0 = 1$ and the eigenvalue $\mu = 4$ is depicted. In the same figure, contour plot of the soliton superimposed on the initial condition and underlying periodic lattice ($N = 4$) is shown. Fig.(2.3) and Fig.(2.4) display the same outcomes for Penrose-5 and Penrose-7 potentials respectively. Note that for each case, the initial condition is taken on the lattice maximum and after the iteration, a localized mode is obtained at the same location.
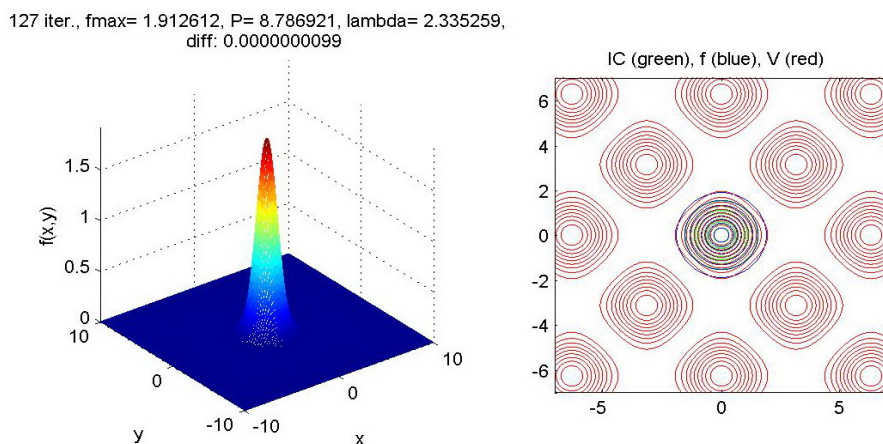
Figure 2.2: 3D view of the soliton on the periodic lattice maximum with $e_0 = 8$, $V_0 = 1$ and $\mu = 4$ and its contour plot superimposed on the initial condition and underlying lattice ($N = 4$)
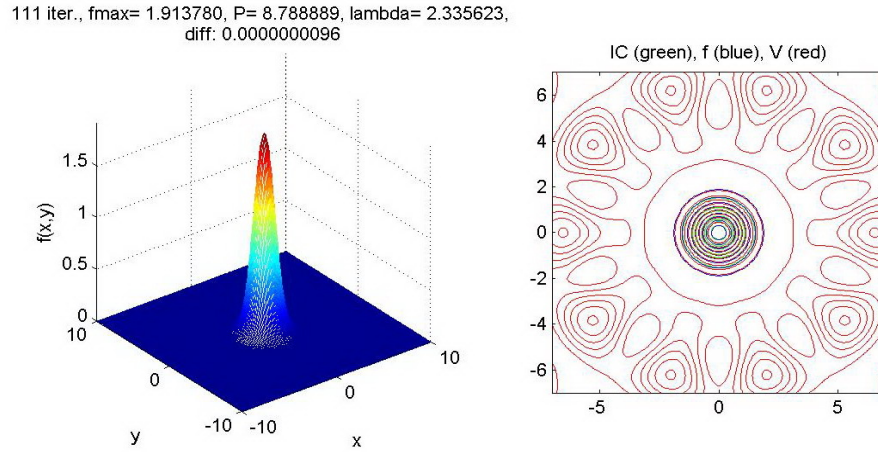
Figure 2.3: 3D view of the soliton on the Penrose-5 lattice maximum with $e_0 = 8$, $V_0 = 1$ and $\mu = 4$ and its contour plot superimposed on the initial condition and underlying lattice ($N = 5$)
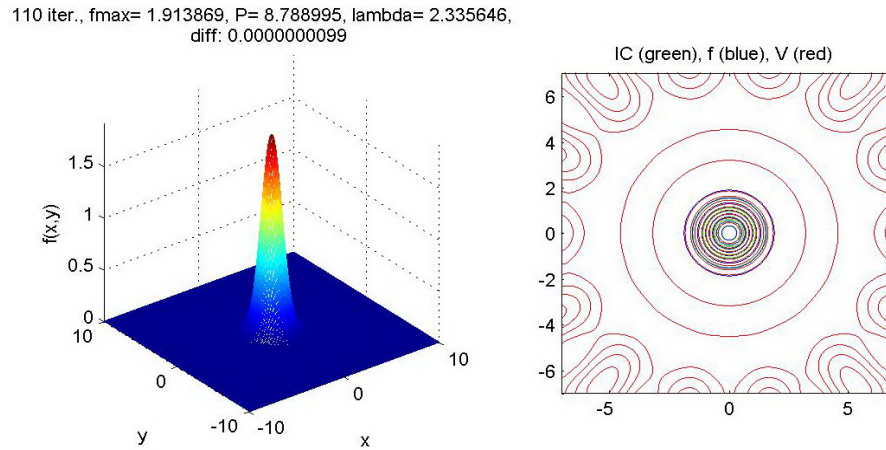
Figure 2.4: 3D view of the soliton on the Penrose-7 lattice maximum with $e_0 = 8$, $V_0 = 1$ and $\mu = 4$ and its contour plot superimposed on the initial condition and underlying lattice ($N = 7$)

2.2.2 Solitons on lattice minimum

In this subsection, solitons located on the minima of the periodic and Penrose-7 lattices are demonstrated.

In Fig.(2.5), 3D view of the soliton obtained on the lattice minimum with the parameters $e_0 = 8$, $V_0 = 1$ and $\mu = 2.5$ and its contour plot superimposed on the initial condition and the underlying periodic lattice ($N = 4$) is plotted. Fig.(2.6) displays the same outcome for Penrose-7 potential. Note that for each case, the initial condition is taken on the lattice minimum and after the iteration, a localized mode is obtained at the same location.
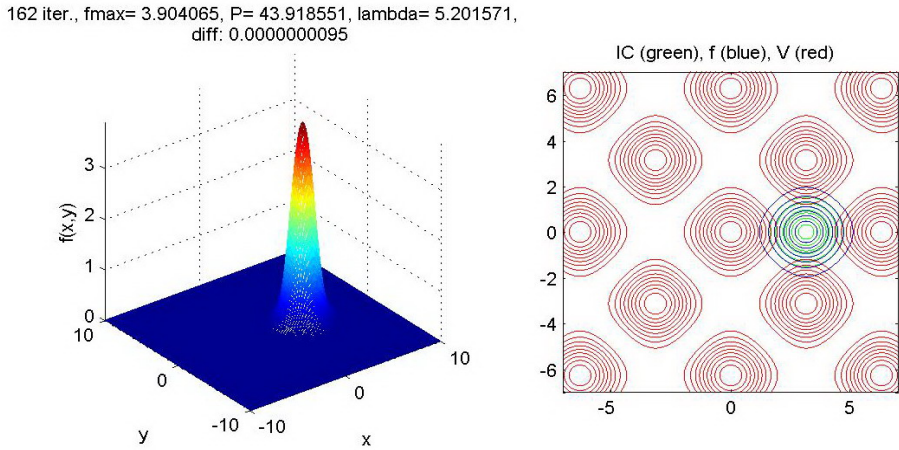
13

162 iter., fmax= 3.904065, P= 43.918551, lambda= 5.201571,
diff: 0.0000000095

IC (green), f (blue), V (red)

Figure 2.5: 3D view of the soliton obtained on the periodic lattice minimum with
$e_0 = 8$, $V_0 = 1$ and $\mu = 2.5$ and its contour plot superimposed on the initial
condition and the underlying lattice ($N = 4$)

96 iter., fmax= 4.065793, P= 45.618991, lambda= 5.309544,
diff: 0.0000000069

IC (green), f (blue), V (red)

Figure 2.6: 3D view of the soliton obtained on the Penrose-7 lattice minimum with
$e_0 = 8$, $V_0 = 1$ and $\mu = 2.5$ and its contour plot superimposed on the initial
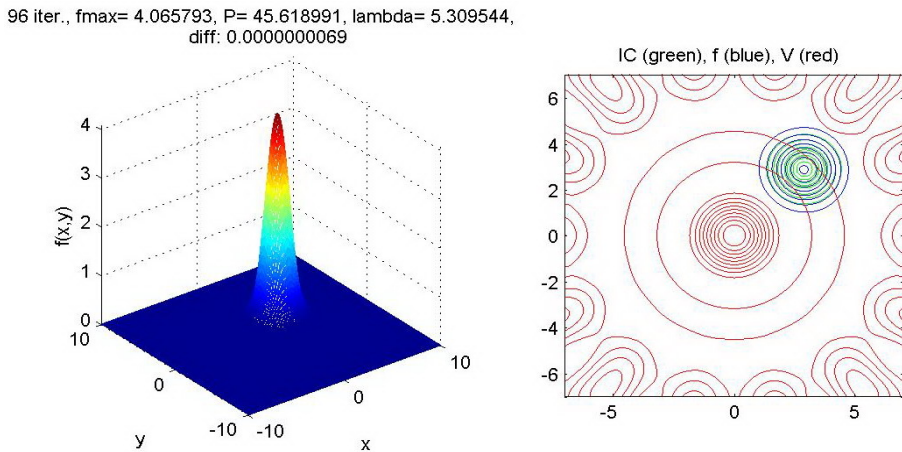condition and the underlying lattice ($N = 7$)

2.2.3 Comparison of fundamental solitons

In order to compare the maximum amplitudes and the profiles of the fundamental
solitons obtained on the periodic, Penrose-5 and Penrose-7 lattices, on axis mode
profiles are depicted in Fig.(2.7).

It can be observed from Fig.(2.7) that the amplitudes of the fundamental solitons slightly
increase as the numerical value of N increases. On the other hand, the shapes of the
fundamental solitons do not exhibit any difference as N increases despite the fact that
the fundamental lattice solitons in Kerr medium show changes in shape. For example,
Penrose-5 solitons are shown to have dimples when their eigenvalues are close to gap
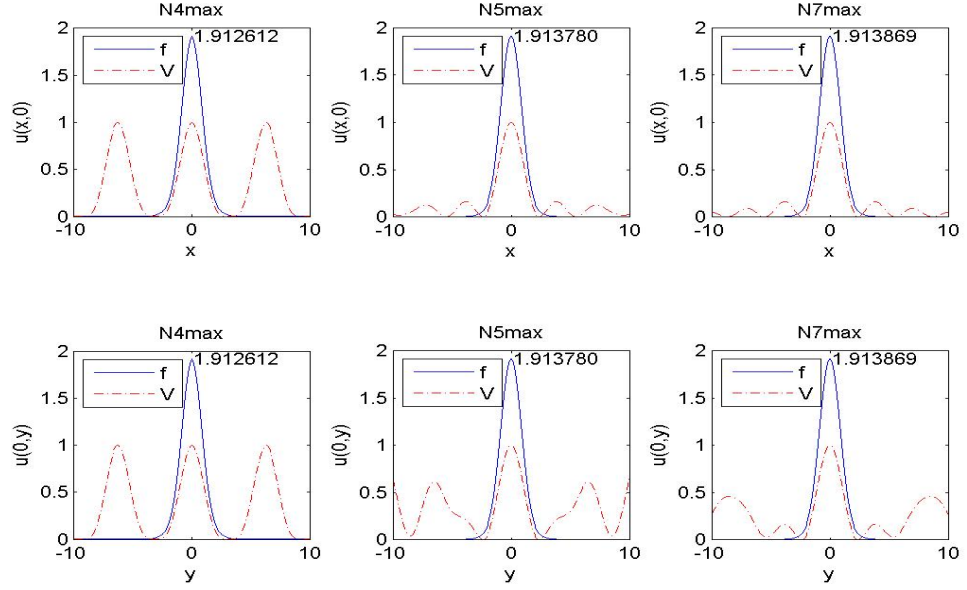edge [8].

14

Figure 2.7: On axis profiles of the solitons obtained with $e_0 = 8$, $V_0 = 1$ and $\mu = 4$ at the maximum of the potentials, $N = 4$, $N = 5$ and $N = 7$ along x-axis (upper row) and y-axis (lower row)

In order to investigate the effect of the potential depth (V_0) on the fundamental solitons, the periodic lattice case is considered and it is shown that the amplitude of the fundamental soliton located on the lattice maximum decreases as the potential depth increases. An example for this fact is illustrated in Fig.(2.8) where $N = 4$ (periodic lattice) and V_0 is increased from 1 to 4.

2.3 Band-gap Structures of Fundamental Lattice Solitons

Band-gap structure is a linear concept that first appeared in Floquet theory as well as condensed matter theory (i.e. diffraction of X-rays through atomic crystals).

In nonlinear optics, the propagation of the soliton on a lattice depends on the depth of the lattice and the propagation constant (or the eigenvalue). In the spectrum of the propagation, there are strips (or regions), where a localized structure is obtained (called *gap*s) and strips where the solution is not a localized structure but an extended state (called *band*s). The whole spectrum is called *band-gap structure* of the lattice or the potential.

The first nonlinear gap of a lattice is the region where localized solutions (solitons) exist. In a certain parameter regime of the potential depth V_0 and the propagation constant μ,
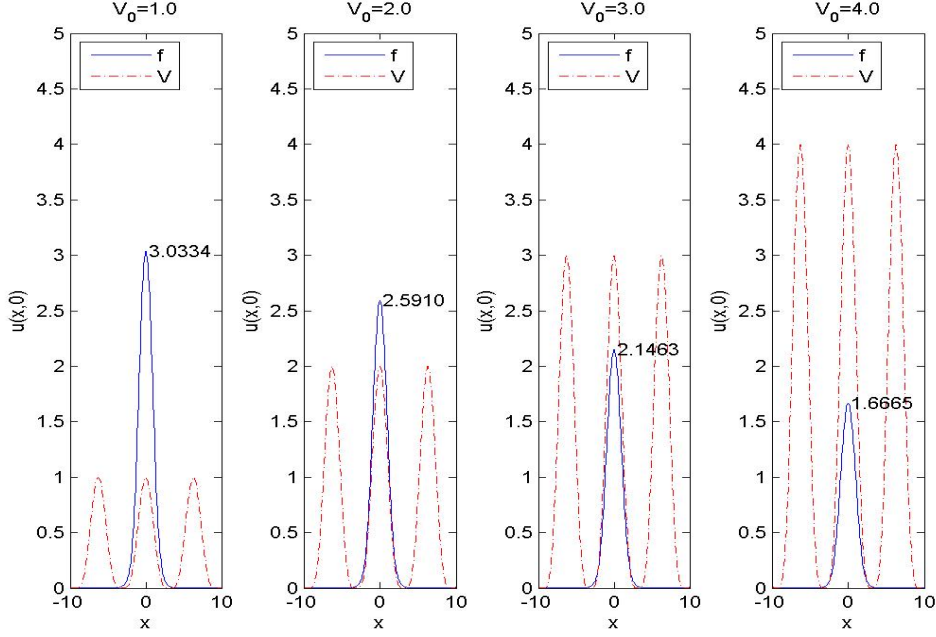
Figure 2.8: On axis profiles of the solitons obtained with $e_0 = 8$, $V_0 = 1, 2, 3, 4$ and $\mu = 3$ at the maximum of the periodic potential ($N = 4$) along x-axis
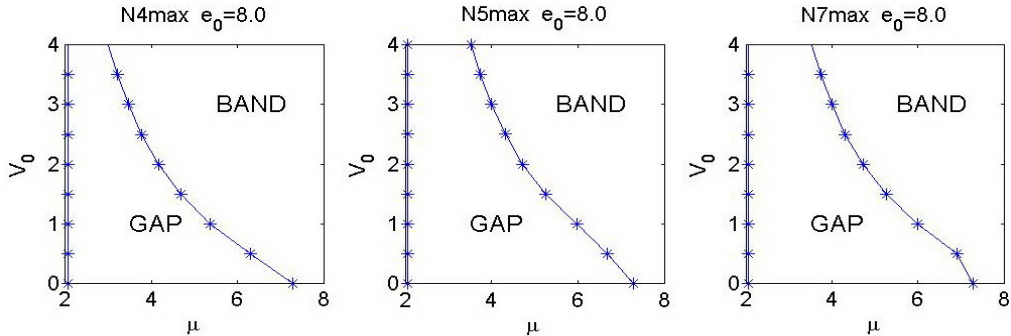

Figure 2.9: Band-gap structure of the solitons obtained with $e_0 = 8$ and the potentials $N = 4, N = 5$ and $N = 7$ at the lattice maximum

spectral renormalization method converges to a localized bound state, i.e. to the solution of (**1.1**) that is bounded and decays to zero. By fixing the potential depth and increasing the eigenvalue, both the convergence and the localization of the solution are checked. In this way, the first nonlinear gap edge of the lattices considered in this work is obtained. Beyond a certain threshold value of the eigenvalue μ, the numerical method yields a Bloch wave.

In Fig.(2.9), the band-gap structures are depicted for periodic, Penrose-5 and Penrose-7 solitons in separate graphs, located on the (absolute) lattice maxima for the fixed value of $e_0 = 8$. For a more clear comparison of the band-gap structures, those obtained band-gap structures are depicted on top of each other in Fig.(2.10).
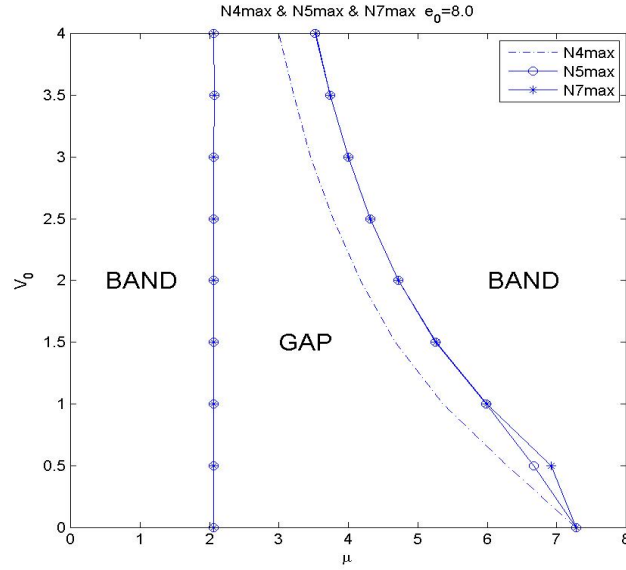
Figure 2.10: Band-gap structure of the solitons obtained with $e_0 = 8$ and the potentials $N = 4$, $N = 5$ and $N = 7$ at the lattice maximum (superimposed)
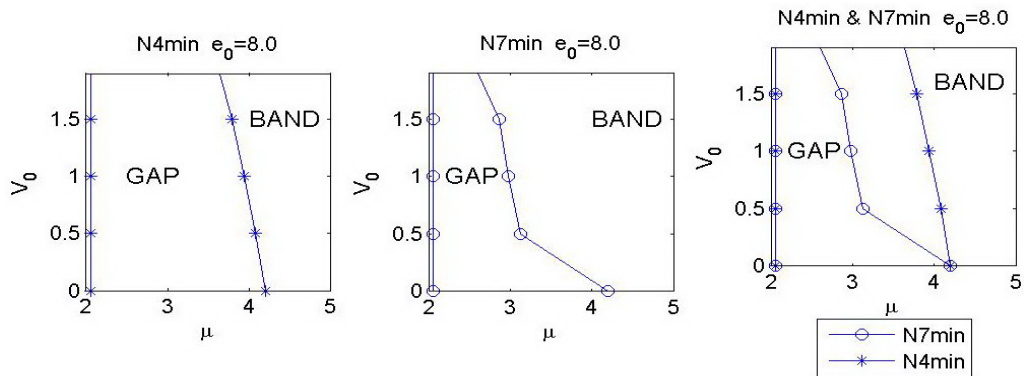
Figure 2.11: Band-gap structure of the solitons obtained with $e_0 = 8$ and the potentials $N = 4$ and $N = 7$ at the lattice minimum

In Fig.(2.11), the band-gap structures are depicted for periodic and Penrose-7 solitons in separate graphs, located on the lattice minima for the fixed value of $e_0 = 8$. For a more clear comparison of the band-gap structures, those obtained band-gap structures are depicted on top of each other in the same figure.

It is observed, especially from the Fig.(2.10), that increasing N expands the gap region. This shows the fact that the gap regions are wider for quasicrystal type lattices than that of the periodic type lattice.

Figure 2.12: Gap width versus e_0 graph of the solitons obtained with $V_0 = 1$ and the potential ($N = 4$) at the lattice maximum and minimum

Figure 2.13: Gap width versus e_0 graph of the solitons obtained with $V_0 = 1$ and the Penrose type potentials ($N = 5$ and $N = 7$) at the lattice maximum and minimum
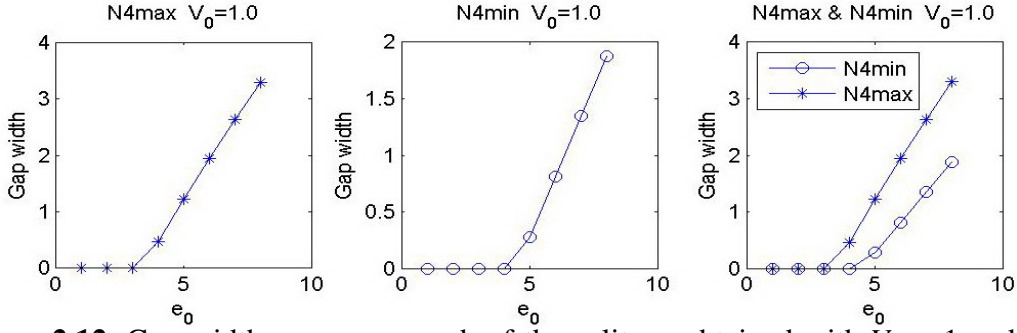
2.4 The Effect of e_0 on the Gap Width

In this subsection, the effect of the saturation parameter e_0 that appears in the saturable NLS equation is investigated. In order to observe this effect, the potential depth $V_0 = 1$ is fixed and by the use of the SR method, the existence of fundamental solitons for increasing values of e_0 for the periodic, Penrose-5 and Penrose-7 lattices are checked.

For small e_0 values, no soliton could be obtained. As e_0 gets greater, the number of eigenvalues for which a soliton exists increases. In other words, the gap width increases as e_0 increases. It is also to be noted that for the same e_0 value, the gap width of the solitons on the lattice maximum is greater than the gap width of the solitons on the lattice minimum.

Above mentioned facts are demonstrated in Fig.2.12 and 2.13.

Figure 2.14: Gap width versus V_0 graph of the solitons obtained with $e_0 = 8$ and the potential ($N = 4$) at the lattice maximum and minimum
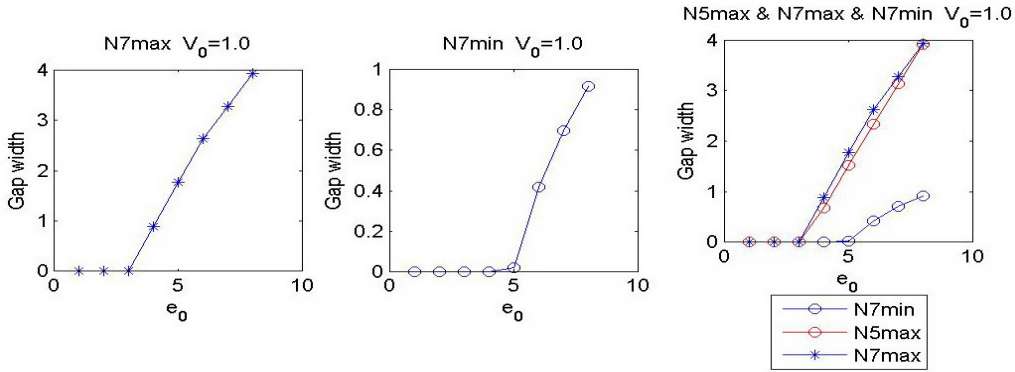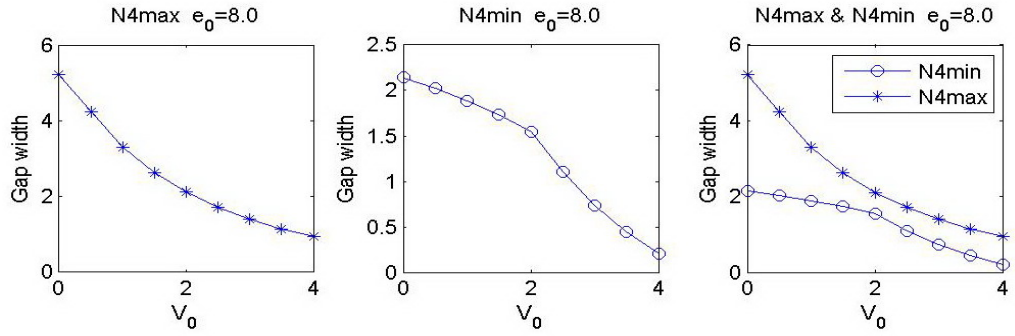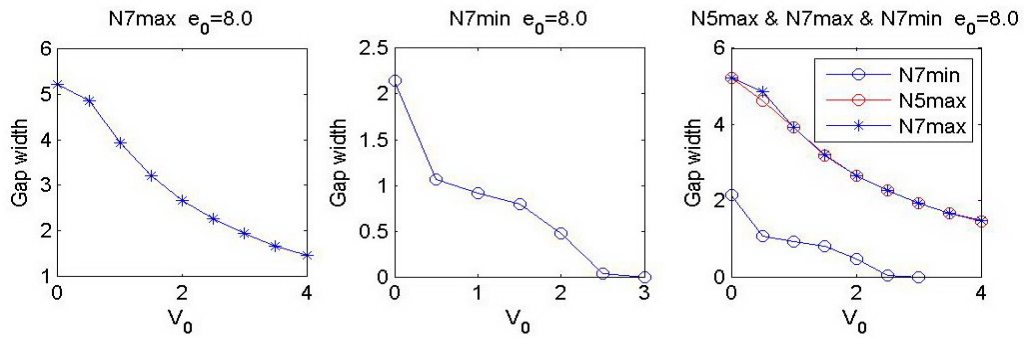

Figure 2.15: Gap width versus V_0 graph of the solitons obtained with $e_0 = 8$ and the Penrose type potentials ($N = 5$ and $N = 7$) at the lattice maximum and minimum

2.5 The Effect of V_0 on the Gap Width

In this subsection, the effect of the potential depth on the gap width is investigated. In order to explore this phenomenon, the potential depth V_0 versus gap width graphs for the periodic potential $N = 4$ is plotted. Those graphs for fundamental solitons on lattice maximum and minimum are shown in Fig.(2.14). In both cases, it can be seen that the gap width decreases as V_0 increases. Same phenomenon occurs for quasicrystals as well. In Fig.(2.15), it is shown that the gap width decreases as V_0 increases for Penrose-7 solitons located both on lattice maxima and minima. In the same figure, V_0 versus the gap width graph for Penrose-5 solitons on lattice maximum is also plotted and it can be seen that for the same V_0 value, the gap width of the solitons located on the lattice maximum are greater than the gap width of the solitons located on the lattice minimum.

19

2.6 The Effect of the Potential Type on the Gap Width

When the figures 2.9 and 2.10 are considered, it is observed that the Penrose-7 type potential brings out a bigger gap region than the Penrose-5 type potential and the Penrose-5 type potential brings out a bigger gap region than periodic $N = 4$ type potential. This holds also true for other cases, i.e. for different e_0 values. So, one can claim that the gap widths increase as N increases.

3. NONLINEAR STABILITY ANALYSIS OF FUNDAMENTAL SOLITONS

In this section, the nonlinear stability properties of the fundamental lattice solitons are explored. One way to do this is the power analysis. The *power* is defined as

$$P = \int_{-\infty}^{\infty} \int_{-\infty}^{\infty} |f(x,y)|^2 dx dy \tag{3.1}$$

and plays an important role in determining the stability of the soliton $f(x,y)$. In [26], Vakhitov and Kolokolov proved that a necessary condition for the linear stability of the soliton $f(x;\mu)$ is

$$\frac{dP}{d\mu} < 0 . \tag{3.2}$$

In other words, the soliton is stable only if its power decreases with increasing propagation constant μ. This condition is called the *slope condition*.

Key analytic results on nonlinear stability were obtained in [27, 28]. They proved that the necessary conditions for nonlinear stability are the slope condition (**3.2**) and the spectral condition. Furthermore, it is well known that a necessary condition for collapse in the 2D cubic NLS equation is that the power of the beam exceeds the critical power $P_c \approx 11.7$ [29].

The fundamental solitons of the NLS equation can become unstable in two ways:

1. Is the slope condition not satisfied, this leads to a *focusing instability*.

2. Is the spectral condition associated with the eigenvalue problem (see [30]) not satisfied, this leads to a *drift instability*.

In order to investigate the nonlinear stability, first approach is trying to predict collapse by using the VK criterion by plotting the soliton power P versus the propagation constant μ graph.

As it can be seen from figures 3.1 and 3.2, no matter whether the soliton is located on a lattice maximum or minimum, the power decreases as μ increases for all three different potentials. Consequently, all the solitons obtained from the numerical solution
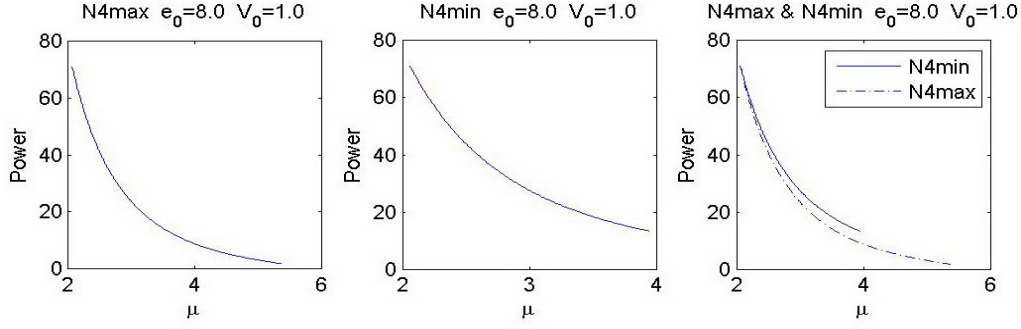
Figure 3.1: Power versus μ graph of the solitons obtained with $e_0 = 8$, $V_0 = 1$ and the potential ($N = 4$) at the lattice maximum and minimum
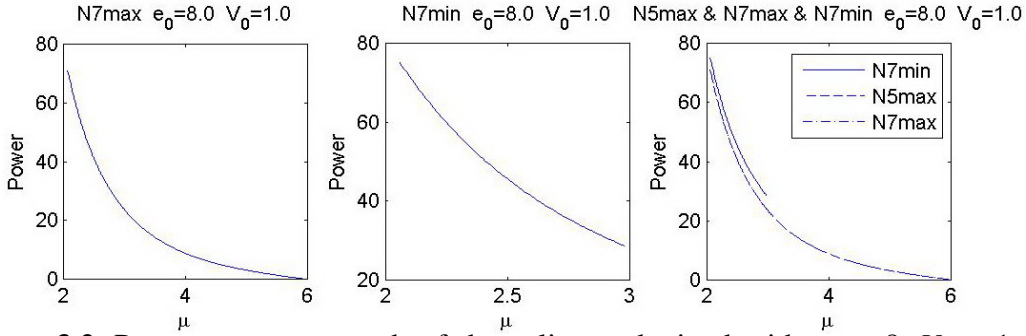

Figure 3.2: Power versus μ graph of the solitons obtained with $e_0 = 8$, $V_0 = 1$ and the Penrose type potentials ($N = 5$ and $N = 7$) at the lattice maximum and minimum

of the Eq.(**1.1**) by the spectral renormalization method explained in the previous section are expected to be stable as they all satisfy the Vakhitov-Kolokolov stability criterion. However, the VK-condition is not sufficient. The soliton may undergo a drift instability, that is, the soliton might move from the lattice maximum towards a nearby lattice minimum during the direct simulation. One way to check this is to let the soliton move along the *z*-axis and see whether it conserves its maximum amplitude and its location.

In this context, the center of mass of a soliton is defined as follows:

$$CM = \frac{1}{P} \int_{-\infty}^{\infty} \int_{-\infty}^{\infty} (x+iy)|f(x,y)|^2 dx dy \tag{3.3}$$

where *P* stands for power.

The *x* and *y* coordinates of the center of mass (CM) are given by

$$<x> = \text{real}(CM)$$
$$<y> = \text{imag}(CM) \ . \tag{3.4}$$

To study whether there exists a drift instability or not, Eq.(**1.1**) is computed over a long distance. For this purpose, a random noise of 1% is added to the soliton; finite difference method is used on derivatives u_{xx} and u_{yy}, and fourth order Runge-Kutta method is employed to advance in z.

A fundamental soliton is considered nonlinearly stable if it conserves its location and maximum amplitude during the direct simulation. Therefore, the maximum amplitude and centers of mass versus the propagation distance graphs are plotted for the fundamental solitons. Solitons located on lattice maxima and minima are investigated separately.

3.1 Stability Analysis of Solitons on Lattice Maximum

Following are sample outcomes of the nonlinear stability test for some parameters and different potentials. More precisely, Fig.(3.3) depicts the evolution of the soliton obtained on the lattice maximum of the periodic potential ($N = 4$) with $e_0 = 8$, $V_0 = 1$ and $\mu = 4$, the change of x and y coordinates of the center of mass over z, cross section

Figure 3.3: Evolution of the soliton obtained with $e_0 = 8$, $V_0 = 1$, $\mu = 4$ and the potential $N = 4$. (a) Peak amplitude $max_{x,y}|u(x,y,z)|$ as a function of the propagation distance z, (b) Change of x and y coordinates of the center of mass over z, (c) Cross section along the diagonal axis of the soliton at the maximum superimposed on the potential $N = 4$ at $z = 10$, (d) Contour plot of the soliton at the maximum superimposed on the potential $N = 4$ at $z = 10$.

23

Figure 3.4: Same as Fig.(3.3) with $N = 5$

along the diagonal axis of the soliton superimposed on the potential at $z = 10$ and contour plot of the soliton superimposed on the potential after the propagation; Fig.(3.4) and Fig.(3.5) depict the same but for the Penrose-5 and Penrose-7 potentials respectively. Note that for each case, the initial condition is taken on the lattice maximum, so are the obtained solitons.

As it can be seen from figures 3.3, 3.4 and 3.5, peak amplitudes of the fundamental solitons slightly oscillate with the propagation distance z and the centers of mass almost stay at the same place. This suggests that the fundamental solitons for all three lattices are nonlinearly stable.

In contrary, the existence of nonlinearly unstable solitons of the NLS equation with Kerr nonlinearity for the periodic potential $N = 4$ and Penrose-5 potential were shown in [8] and for the Penrose-7 potential in [18].

3.2 Stability Analysis of Solitons on Lattice Minimum

Following are sample outcomes of the nonlinear stability test for some parameters and different potentials. More precisely, Fig.(3.6) depicts the evolution of the soliton obtained on the lattice minimum of the periodic potential ($N = 4$) with $e_0 = 8$, $V_0 = 1$ and $\mu = 2.5$, the change of x and y coordinates of the center of mass over z, cross
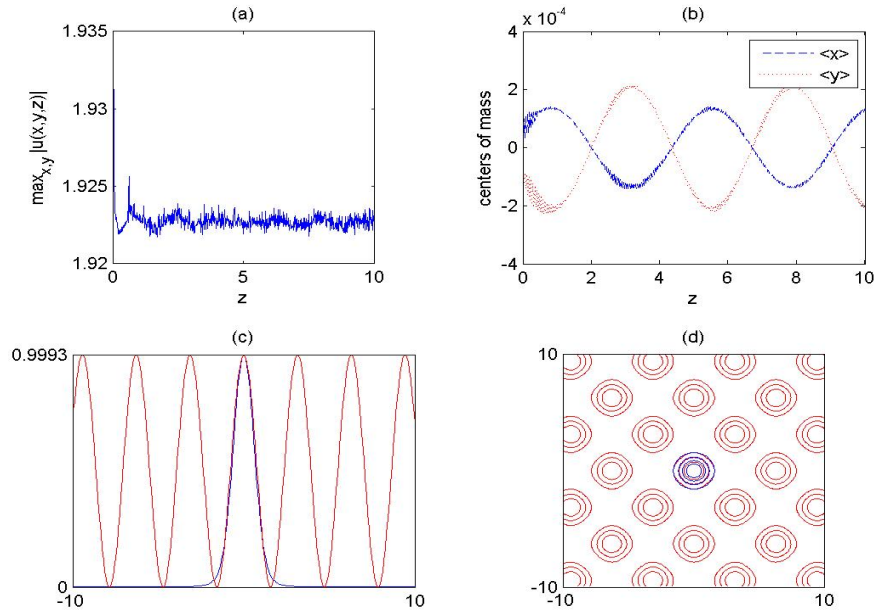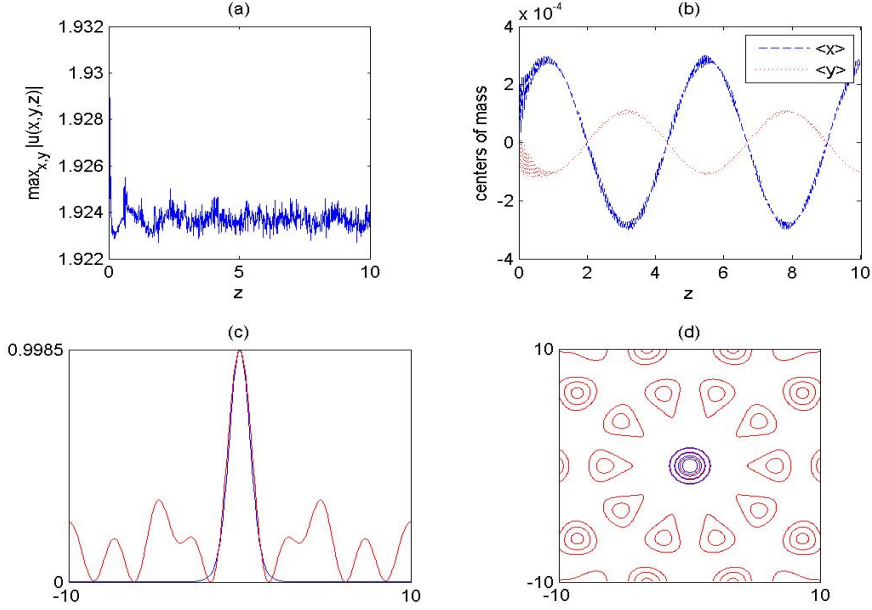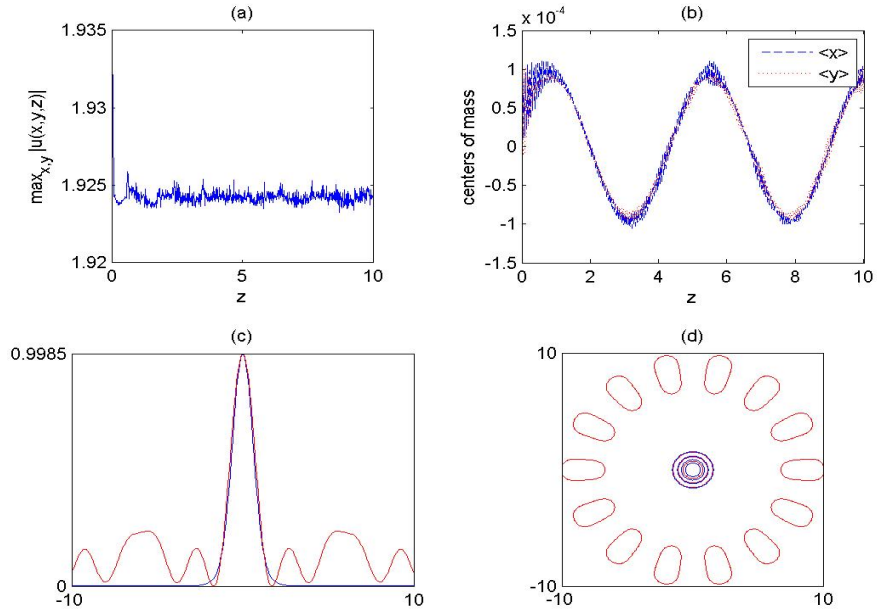
24

Figure 3.5: Same as Fig.(3.3) with $N = 7$

section along the diagonal axis of the soliton superimposed on the potential at $z = 10$ and contour plot of the soliton superimposed on the potential after the propagation; Fig.(3.7) depicts the same but for the Penrose-7 potential. Note that for each case, the initial condition is taken on the lattice minimum, so are the obtained solitons.

As it can be seen from Fig.(3.6), peak amplitude of the fundamental soliton on periodic lattice slightly oscillates with the propagation distance z and the center of mass almost stays at the same place. This suggests that the fundamental soliton on the periodic lattice minimum is nonlinearly stable.

However, the soliton obtained at the minimum of the Penrose-7 potential is not stable. The drift instability can be clearly seen in Fig.(3.7b) by the change of the center of mass. If the positions of the soliton before (Fig.(2.6)) and after (Fig.(3.7d)) the propagation are compared, it can be said that the soliton moves from one minimum over the absolute maximum to another minimum. This also explains the big difference in the change of the amplitude in the middle of the graph in Fig.(3.7a).
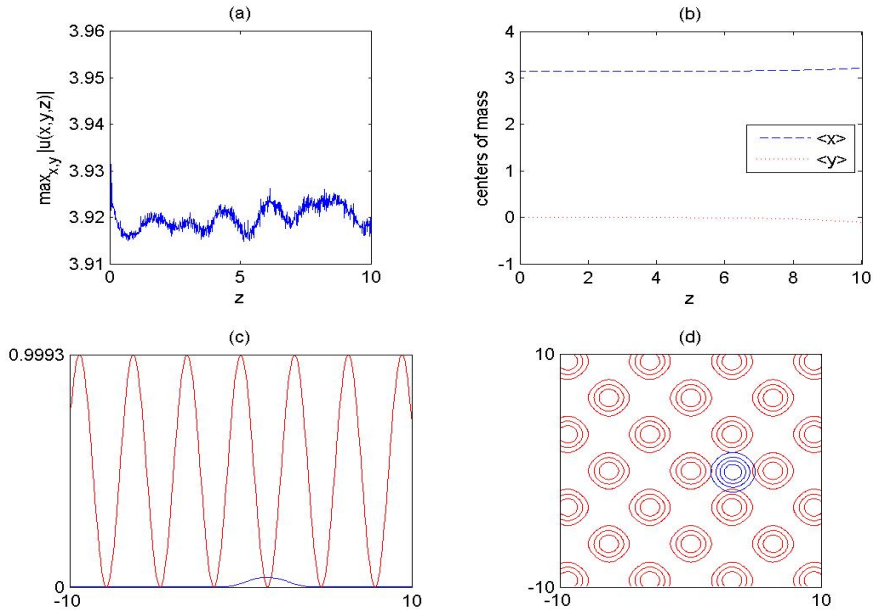
Figure 3.6: Evolution of the soliton obtained with $e_0 = 8$, $V_0 = 1$, $\mu = 2.5$ and the potential $N = 4$. (a) Peak amplitude $max_{x,y}|u(x,y,z)|$ as a function of the propagation distance z, (b) Change of x and y coordinates of the center of mass over z, (c) Cross section along the diagonal axis of the soliton at the maximum superimposed on the potential $N = 4$ at $z = 10$, (d) Contour plot of the soliton at the minimum superimposed on the potential $N = 4$ at $z = 10$.

Figure 3.7: Same as Fig.(3.6) with $N = 7$

26

4. CONCLUSION AND RECOMMENDATIONS

The purpose of this study was to investigate the existence and stability properties of solitons in periodic ($N = 4$) and certain quasicrystal ($N = 5$ and $N = 7$) lattices.
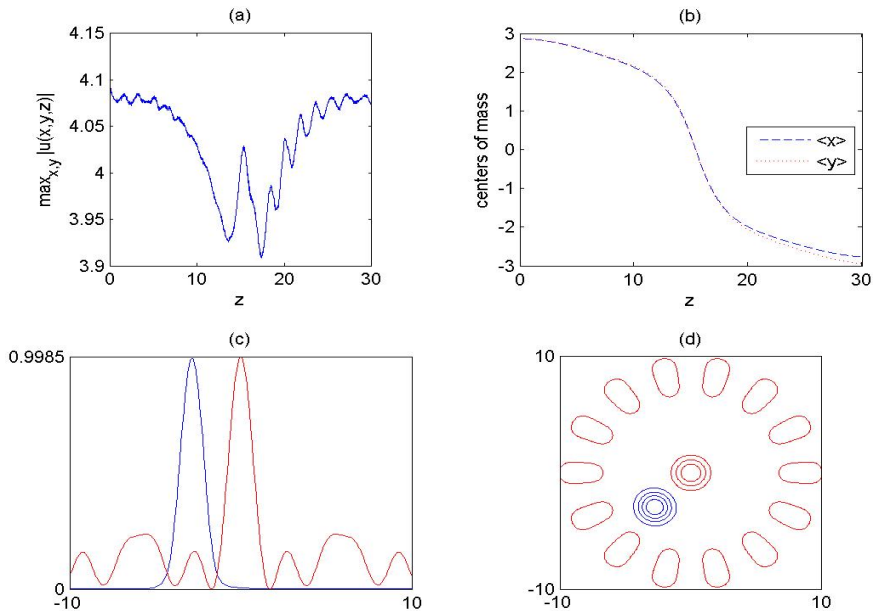
Firstly, the solutions of saturable NLS equation with an external potential are obtained by means of the spectral renormalization method. The band-gap structure of the lattice solitons are obtained for periodic and Penrose type potentials. The effects of the saturation parameter e_0 and the potential depth V_0 on the gap width are investigated and depicted in some figures and it is shown that on one hand, increasing the saturation parameter e_0 expands the gap width, on the other hand, increasing the potential depth V_0 decreases the gap width. Another result is that increasing N expands the gap width.

After obtaining fundamental solitons, their nonlinear stability properties are investigated according to Vakhitov-Kolokolov stability criterion and by direct simulations. It is observed that direct simulations are in good agreement with Vakhitov-Kolokolov stability criterion.

As a future study, the linear stability properties of the fundamental solitons can be explored and those results can be compared with the linear eigenvalue problem.

REFERENCES

[1] **Christodoulides, D. N., Lederer, F., Silberberg Y.**, 2003. Discretizing light behaviour in linear and nonlinear waveguide lattices, *Nature*, **424**, 817.

[2] **Chen, Z., Kivshar, Y. S., Martin, H., Neshev, D.** , 2004. Soliton stripes in two-dimensional nonlinear photonic lattices, *Opt. Lett.* , **29**, 486.

[3] **Blech, I., Cahn, J. W., Gratias, D., Shechtman D.**, 1984. Metallic phase with long-range orientational order and no translational symmetry, *Phys. Rev. Lett.*, **53**, 1951.

[4] **Marder, M. P.**, 2000. *Condensed Matter Physics*, Wiley, New York.

[5] **Chen, Z., Fedele, F., Yang, J.**, 2005. Properties of defect modes in one-dimensional optically induced photonic lattices, *Stud. Appl. Math.*, **115**, 279.

[6] **Buljan, H. et al.**, 2005. Partially coherent waves in nonlinear periodic lattices, *Stud. Appl. Math.*, **115**, 173.

[7] **Raffaella, P., Roberta, F., Russell, J.**, 2002. On the nature of the spectrum of the quasi-periodic Schrödinger operator, *Nonlinear Analysis : Real World Applications*, **3**, 37.

[8] **Ablowitz, M. J., Antar, N., Bakırtaş, İ., Ilan, B.**, 2010. Band-gap boundaries and fundamental solitons in complex two-dimensional nonlinear lattices, *Phys. Rev.* A **81**, (3) 033834.

[9] **Ablowitz, M. J. et al.**, 2006. Solitons in two-dimensional lattices possessing defects, dislocations, and quasicrystal structures, *Physical Review E*, **74**, 035601(R).

[10] **Lomdahl, P. S.**, 1984. What is a soliton?, *Los Alamos Science*.

[11] **Senechal, M.**, 2006. What is a quasicrystal?, *Notices of the AMS*, **53**, 8.

[12] **Freedman, B. et al.**, 2000. Wave and defect dynamics in nonlinear photonic quasicrystals, *Nature*, **440**, 1166.

[13] **Myint-U, T.**, 1987. *Partial Differential Equations for Scientists and Engineers*, p. 318-322, Prentice-Hall, New Jersey.

[14] **Berge, L.**, 1998. Wave collapse in physics: principles and applications to light and plasma waves, *Phys. Rep.*, **303**, 260.

[15] **Kelley, P. L.**, 1965. Self-focusing of optical beams, *Phys. Rev. Lett.*, **15**, 1005-1008.

[16] **Fibich, G., Papanicolaou, G. C.**, 1999. Self-focusing in the perturbed and unperturbed nonlinear Schrödinger equation in critical dimension, *SIAM J. Appl.Math.*, **60**, 183-240.

[17] **Fibich, G., Papanicolaou, G. C.**, 1998. A modulation method for self-focusing in the perturbed critical nonlinear Schrödinger equation, *Phys. Lett. A*, **239**, 167-173.

[18] **Bağcı, M.**, 2010. Fundamental Solitons in Complex Two Dimensional Lattices, *M.Sc. Thesis*, İTÜ Institute of Science and Technology, Istanbul.

[19] **Segev, M., Stegeman, G. I.**, 1999. Optical spatial solitons and their interactions: universality and diversity, *Science*, **286**, 1518.

[20] **Ablowitz, M.J., Horikis, T. P.**, 2010. Nonlinear waves in optical media, *J. Comp. Appl. Math.*, **234**, 1896.

[21] **Yang, J.**, 2004. Stability of vortex solitons in a photorefractive optical lattice, *New Journal of Physics*, **6**, 47.

[22] **Akhmediev, N. N., Soto-Crespo, J. M., Wright, E. M.**, 1992. Recurrence and azimuthal-symmetry breaking of a cylindrical Gaussian beam in a saturable self-focusing medium, *Phys. Rev. A*, **45**, 3168.

[23] **Edmundson, D. E., Enns, R. H.**, 1992; 1993; 1995. Particlelike nature of colliding three-dimensional optical solitons, *Opt. Lett.*, **17**, 586; **18**, 1609; *Phys. Rev. A*, **51**, 2491.

[24] **Petviashvili, V. I.**, 1976, *Plasma Phys.*, **2**, 469.

[25] **Ablowitz, M. J., Musslimani Z. H.**, 2005. Spectral renormalization method for computing self-localized solutions to nonlinear systems, *Opt. Lett.*, **30**, 2140.

[26] **Kolokolov, A., Vakhitov, M.**, 1973. *Radiophys. Quantum Electron*, **16**, 783.

[27] **Weinstein, M. I.**, 1985. *SIAM J. Math. Anal.*, **16**, 3.

[28] **Rose, H. A., Weinstein, M. I.**, 1988. *Physica D*, **30**, 207.

[29] **Weinstein, M. I.**, 1982. *Commun. Math. Phys.*, **87**, 567.

[30] **Sivan Y. et al.**, 2008. Qualitative and quantitative analysis of stability and instability dynamics of positive lattice solitons, *Physical Review E*, **78**, 046602.

CURRICULUM VITAE

Candidate's full name: İzzet GÖKSEL

Place and date of birth: Şişli, 23.05.1985

Permanent Address: Konaklar Mah. Söğüt Sok.
No:3 9/29 TR-34330
Yeni Levent, İstanbul

Universities and Colleges attended:

- Istanbul Technical University,
  Mathematical Engineering - M.Sc. 2009-2011
  Computer Engineering   - B.Sc. 2006-2007, 2008-2010
  Mathematical Engineering - B.Sc. 2005-2007, 2008-2009

- University of Nantes (France),
  Mathematical Engineering - Erasmus 2007-2008

- Istanbul (Erkek) Lisesi (Deutsche Auslandsschule)
  1996-2002, 2003-2005

- Robert E. Lee High School (Tyler, USA) 2002-2003

Publications:

- Yüksel, B., Oktuğ, S., Karabulut-Kurt, G., **Göksel, I.**, 2010: An Empirical Study on The Effect of Mobility of GSM Telephone Traffic, *Proc. of IEEE PIMRC*, September 2010, Istanbul, Turkey.